

Dynamic light scattering from pulsatile flow in the presence of induced motion artifacts

M. Nemati,^{1,*} C. N. Presura,² H. P. Urbach,¹ and N. Bhattacharya¹

¹ *Optics Research Group, Department of Imaging Science and Technology, Delft University of Technology, Lorentzweg 1, 2628 CJ Delft, The Netherlands*

² *Philips Research, High Tech Campus 34, 5656AE Eindhoven, The Netherlands*

* m.nemati@tudelft.nl

Abstract: Continuous health monitoring has become a major theme of our aging society. Portable devices play an important role here. Many optical portable devices are susceptible to motion induced artifacts. We have performed an experimental study for detection of fluid pulsation based on multi-exposure speckle images, in presence of motion induced artifacts. Induced motion of a wide range of frequencies and amplitudes were generated to resemble sensor motion with respect to skin. The data was analyzed using speckle contrast and correlation. We concluded that both techniques have their own advantages, depending on the measurement configuration. A study of angles between illumination and detection revealed that larger angles yields better signal. Shorter exposure time was more successful in extracting the signal. We also performed in-vivo measurements that agree with the in-vitro case. We also show that a minimum collection of two pixels from the speckle image is sufficient to extract relevant results.

© 2014 Optical Society of America

OCIS codes: (100.0100) Image processing; (170.0170) Medical optics and biotechnology; (230.0230) Optical devices; (290.0290) Scattering.

References and links

1. D. A. Boas and A. K. Dunn, "Laser speckle contrast imaging in biomedical optics," *J. Biomed. Opt.* **15**, 011109 (2010).
2. A. K. Dunn, "Laser speckle contrast imaging of cerebral blood flow," *Ann. Biomed. Eng.* **40**, 367–377 (2012).
3. M. Nemati, L. Wei, M. G. Zeitouny, M. Stijnen, S. van Tuijl, N. Bhattacharya, and H. P. Urbach, "Laser speckle analysis of flow in presence of static scatterers," *Proc. SPIE* **8413**, 84131D–84131D–6 (2012).
4. D. Briers, D. D. Duncan, E. Hirst, S. J. Kirkpatrick, M. Larsson, W. Steenbergen, T. Stromberg, and O. B. Thompson, "Laser speckle contrast imaging: theoretical and practical limitations," *J. Biomed. Opt.* **18**, 66018 (2013).
5. M. Nemati, R. W. C. G. R. Wijshoff, J. M. a. Stijnen, S. van Tuijl, J. W. M. Bergmans, N. Bhattacharya, and H. P. Urbach, "Laser-speckle-based detection of fluid pulsation in the presence of motion artifacts: in vitro and in vivo study," *Opt. Lett.* **38**, 5334–5337 (2013).
6. M. Vegfors, L.-G. Lindberg, P. Å. Öberg, C. Lennmarken, "Accuracy of pulse oximetry at various haematocrits and during haemolysis in an in vitro model," *Med. Biol. Eng. Comput.* **31**, 135–141 (1993).
7. A. G. Gilman, "G proteins: transducers of receptor-generated signals," *Annu. Rev. Biochem.* **56**, 615–649 (1987).
8. M. Michalski, V. Briard, and F. Michel, "Optical parameters of milk fat globules for laser light scattering measurements," *Lait* **81**, 787–796 (2001).
9. R. F. Bonner, R. Nossal, S. Havlin, and G. H. Weiss, "Model for photon migration in turbid biological media," *J. Opt. Soc. Am. A* **4**, 423–432 (1987).
10. P. Shi, V. A. Peris, A. Echiadis, J. Zheng, Z. Yisheng, P. Y. S. Cheang, and S. Hu, "Non-contact reflection photoplethysmography towards effective human physiological monitoring," *J. Med. Biol. Eng.* **30**, 161–167 (2009).

11. J. D. Briers and S. Webster, "Quasi real-time digital version of single-exposure speckle photography for full-field monitoring of velocity or flow fields," *Opt. Commun.* **116**, 36–42 (1995).
 12. M. Draijer, E. Hondebrink, T. van Leeuwen, and W. Steenbergen, "Review of laser speckle contrast techniques for visualizing tissue perfusion," *Lasers. Med.Sci.* **24**, 639–651 (2009).
 13. A.F. Fercher and J.D. Briers, "Flow visualization by means of single exposure speckle photography," *Opt. Commun.* **37**, 326–330 (1981).
 14. R. Bandyopadhyay, A. S. Gittings, S. S. Suh, P. K. Dixon, and D. J. Durian, "Speckle-visibility spectroscopy: A tool to study time-varying dynamics," *Rev. Sci. Instrum.* **76**, 093110 (2005).
 15. K. Schatzel, "Noise on photon correlation data. I. Autocorrelation functions," *Quantum Opt.* **2**, 287–305 (1990).
 16. D. A. Boas and A. G. Yodh, "Spatially varying dynamical properties of turbid media probed with diffusing temporal light correlation," *J. Opt. Soc. Am. A* **14**, 192 (1997).
 17. B. J. Berne and R. Pecora, *Dynamic Light Scattering : With Applications to Chemistry, Biology, and Physics* (Dover Publications, 2000), unabridged ed.
 18. P. A. Bandettini, A. Jesmanowicz, E. C. Wong, and J. S. Hyde, "Processing strategies for time-course data sets in functional MRI of the human brain," *Magn. Reson. Med. Sci.* **30**, 161–73 (1993).
-

1. Introduction

Regular monitoring of the vital parameters of the body is becoming increasingly relevant as population demographics in many countries lean towards aging. The recovery and rehabilitation chances increase significantly with early diagnosis. The ability to monitor physical parameters of the human body non-invasively is critical for cost effective treatment and rehabilitation. Non-invasive monitoring is also preferable since there is no contamination, no infection risk and no discomfort to the patient. Optical methods can contribute here significantly and already many non-invasive techniques have been developed with them. Several optical devices have been proposed and implemented to monitor parameters like blood perfusion, skin ailments, and cardiovascular parameters among others. Monitoring the human heart rate using optical techniques has been successfully implemented in many devices. One common device is the pulse oximeter which monitors pulse rate and the peripheral oxygen saturation (SpO_2) of the patient. However, this and other optical devices still face a major challenge in the form of signal extraction in presence of the measurement errors caused by motion induced artifacts. In this paper, we address this issue and study possible techniques of measuring a pulsatile flow in a noisy environment based on speckle images.

Coherent light falling on a diffuse or irregular surface produces an irregular grainy interference pattern named speckle. The constructive or destructive interference of light when it encounters different path lengths due to surface irregularities or traverses different depths in medium, leads to the dark and light parts of the speckle pattern. Movement in the media or of the media cause the speckle pattern to change. The entire speckle pattern could move, maintaining the speckle correlation, or the speckles could begin to blur due to uncorrelated moving scatterers, resulting in decorrelation of the speckle pattern. Speckle imaging has therefore been intensively investigated for several applications from non-destructive testing to biomedical applications [1]. The ability to quantify the decorrelation in the speckle patterns due to moving scatterers makes speckle imaging a technique that has been used extensively to study flow properties including blood flow in tissue.

The optical properties of tissue have a large impact on laser speckle based imaging, since different layers contribute differently to the reflection, absorption and transmission. The variation of the tissue depending upon the ethnicity, age and health of the subject also contributes to the complexity of standardizing parameters for medical applications. In spite of the contribution of large number of varying static parameters, the time variation in the pattern bears the imprint of the moving scatterers which contribute to the interference pattern making up the speckle pattern. Thus, studying the temporal statistics of the speckle fluctuations yields information about the underlying flowing scatterers. An advantage that speckle based techniques have in

comparison to other optical techniques is that they are not based on actual imaging with all its associated complexities. Speckle based techniques have been used to study *in-vivo* blood flow monitoring quite extensively. In a recent review by Dunn [2], a thorough discussion of laser speckle contrast imaging (LSCI) and complementary techniques like multi-exposure laser speckle contrast imaging (MESI) along with relevant applications can be found. An associated problem is the study of pulsatile flow in presence of static scatterers [3].

However, a recent publication [4] has raised the question of feasibility of measuring hemodynamic parameters in presence of motion induced artifacts using speckle based techniques. This question led to the study of pulsatile flow in the presence of induced motion between the illuminating laser and the flow sample [5]. This work used speckle contrast analysis to retrieve the flow pulsation in face of illumination source oscillation of varying amplitude and frequency. The moving beam spot results in a different region of the sample being illuminated each time, thus altering the path length between the laser beam and the detector. The main motion induced artifact in the signal being measured, arises from the changing light penetration depth at the various positions being illuminated. In this work, we would like to investigate various analysis methodologies to study the effectiveness of these techniques in retrieving the signal in face of moving illumination at varying amplitudes and frequencies. For this, we have studied the effect of artifacts for a wide range of amplitudes and frequencies of the induced motion, for multiple-exposure times of the camera. Speckle images are influenced by the exposure time. Longer exposure times cause averaging of the speckles while shorter exposure times do not catch the blurring effect due to the movement of the scatterers, leading to lower and higher speckle contrast values, respectively. Measurements were also performed to investigate the effect of the angle between illumination and detection.

2. Method and materials

2.1. Experimental setup

To study the effect of motion induced artifacts on pulsatile flow, an experimental setup was built in which controlled motion could be implemented, such that the resulting artifacts in the signal could be studied. In this section, we describe the setup that consists of illumination, the skin-mimicking flow cell and the detection.

2.1.1. Flow cell

The flow cell with its components is shown in Fig 1. As can be seen in the figure, the flow cell consists of a semi-rectangular channel with a length of 20mm and a depth of 1mm to represent a homogeneous, thin layer of flow. The top membrane of the cell is a skin phantom made of Delrin[®] (polyoxymethylene, POM) to mimic the scattering properties of skin [6]. The flow cell can have two configurations depending upon the experimental requirement. The channel can be made flexible, allowing for volume changes with pulsation mimicking blood vessels or being rigid, thus having only velocity changes. This is done by replacing the bottom layer with a flexible silicon membrane or a rigid material. In this experiment, we used a roller pump (Minipuls[®] 3) to generate a pulsatile flow with a controlled frequency in our sample. As a scattering fluid, we used milk to mimic the blood flow, as the fat particles in milk scatter light similar to red blood cells (RBC's) in blood [7, 8].

2.1.2. Measurement setup

A schematic of the measurement setup is shown in Fig. 2(a) and the experimental setup itself in Fig. 2(b) The measurement system is composed of three main parts: illumination, detection and the sample. For illumination, we used a vertical cavity surface emitting laser diode (VCSEL)

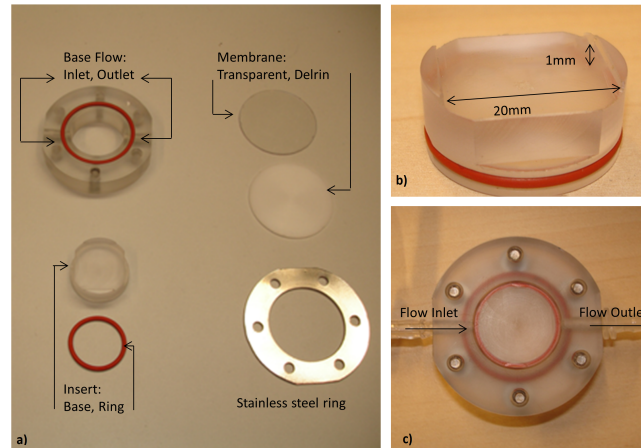


Fig. 1. Flow phantom: a) Components of the flow sample: the base flow cell with the inlet and outlet, the rigid insert that is placed in the base flow cell defining the channel depth, the flow cell membrane which can be either transparent or Delrin and the stainless steel ring which is used in bottom and top to fix the flow cell. b) The insert with the flow channel. c) An assembled version of the flow cell.

with an emission wavelength of 850nm and spectral bandwidth of 0.3nm. The laser diode has a spatial coherence length of 2.4mm and an optical output power of 0.5mW. For our detection system, we used a variable frame rate high speed camera (Photron Fastcam SA3) with the pixel size of $17 \times 17 \mu\text{m}$. For a better magnification, we could couple the camera to a stereomicroscope with overall magnification of 6.4x for the cases, where it is required. The laser can also be mounted at different angles giving us the possibility of changing the angle between the illumination and the camera used for detection. This angle also influences the total area illuminated and the penetration depth, hence the optical path between the source and detector.

To simulate the in-vitro heart rate using the roller pump, we generated fluid pulsation at the rate of 1Hz and 1.25Hz, with an amplitude per stroke of 6.7ml and 7.8ml respectively. The base flow rate for 1Hz and 1.25Hz, was measured to be 40ml/min and 47ml/min respectively.

One main source of artifact is relative motion between the sensor and sample during clinical measurements. To simulate this, the source of illumination can be moved while the camera and sample remain stationary. As can be seen in the setup, Fig 2, the laser diode is attached to the shaker which creates a linear movement. In this case, we use the laser diode as the source of illumination for generating speckle images and at the same time as a source of generating motion induced artifacts. The movement of the shaker causes different parts of the sample to be illuminated, thus creating a different distance between the light source and detector. This causes the optical depth which is traveled through the sample at different locations to change. The banana shape of light path between the source and detector through the sample has its deepest penetration in the middle of the path [9, 10]. With the light source moving, this light banana keeps changing leading to an optical perturbation of the signal from the flowing scatterers which was the main signal being measured. This attempts to imitate the situation in real life when the sensor moves with respect to the skin due to the limb of the patient moving. To generate the motion artifacts, we used a mini-shaker driven by a Labview based program and an amplifier. The shaker moves the laser in the horizontal plane for different frequencies (0.7Hz, 1.4Hz, 2.8Hz, 3.2Hz, 3.6Hz, 4Hz and 4.5Hz) and amplitudes (0.5mm, 1mm, 2mm and 3mm).

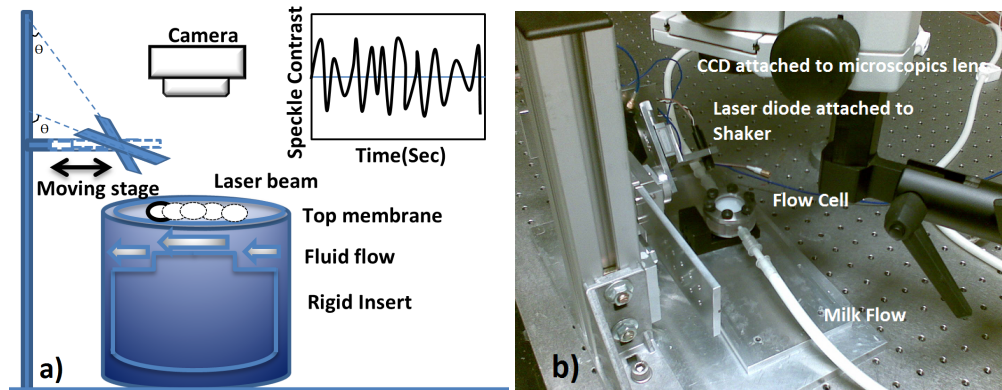


Fig. 2. a) Schematic of the experimental setup and b) The experimental setup. The motion artifacts are generated by the motion of the laser beam which creates a different penetration depth and distance to the detector. The speckle contrast has been calculated over the entire illuminated area.

2.2. Methods

2.2.1. Laser speckle contrast analysis

Laser speckle imaging has the advantage of evaluating the sample without scanning or imaging in a simple and inexpensive apparatus. One of the approaches for analyzing the time fluctuation dynamics of speckle images, is based on the laser speckle contrast which was first introduced by Briers and Webster [11]. In this paper, the time integrated speckle images have been recorded using a single photograph with a specific exposure time. The speckles appear blurry due to longer integration time compared to the speckle decorrelation time. This blurry effect is quantified by the contrast term (K) which is defined as the ratio of the standard deviation (σ) over the average ($\langle I \rangle$), of the intensity fluctuations,

$$K = \frac{\sigma}{\langle I \rangle}. \quad (1)$$

The calculated contrast would have a lower value in case of a sample which has moving scatterers due to the fact that the standard deviation of the intensity would decrease while the average intensity remains constant. The main schemes of computing the speckle images from the raw data are considered as temporal, spatial or a combination of these two. A more detailed description can be found in reference [12].

For each individual measurement, we captured a time sequence of images and calculated the speckle contrast for each image with a spatial window size of 7×7 camera pixels. The resulting contrast time series was then Fourier transformed to obtain the frequency spectrum of the speckle contrast due to fluctuations arising due to different processes, for the entire duration of each measurement.

2.2.2. Correlation based analysis

In a dynamic sample with scattering particles, the measured light intensity will vary over time as particles diffuse in random directions. A quantitative measure of this fluctuation can be obtained by defining a statistical average of the temporal field correlation $g_1(\tau)$ which expresses the displacement of moving particles being integrated over time

$$g_1(\tau) = \frac{1}{T} \int_{-\infty}^{+\infty} E^*(t)E(t+\tau)d\tau. \quad (2)$$

Here τ is the correlation time, T is the exposure time of the image, $E(t)$ is the time dependent electric field and $E^*(t)$ is the complex conjugate of $E(t)$. In fact, there is a relation between the measured speckle contrast mentioned earlier and the correlation function which is better known as the correlation time in the flow analysis. The correlation time, (τ), is the actual decay time of the autocorrelation function which is related to the velocity of the scatterers. The velocity is, in turn, dependent on the scatterer distributions. However, to relate it to the speckle contrast, based on speckle statistics there is a relation between the contrast K^2 , and the time averaged autocorrelation, $g_1(\tau)$, of the intensity fluctuations [13]. The relation has been further improved, [14], by considering the triangular averaging of the correlation function [15],

$$K^2(T) = \frac{2}{T} \int_0^T \beta |g_1(\tau)|^2 (1 - \frac{\tau}{T}) d\tau. \quad (3)$$

Here β is the coherence factor and is dependent on the measurement setup and the laser stability. In an ideal situation, it can be assumed to be equal to one [16]. Instead of measuring the complex field which is the result of superposition of many other fields arriving at the detector, we record the speckle intensities. The field correlation is related to the temporal autocorrelation intensity, $g_2(\tau)$, as expressed by the Sigert relation [17],

$$g_2(q, \tau) = 1 + \beta |g_1(q, \tau)|^2, \quad (4)$$

where q represents the space coordinate. There are theoretical models which associate the measured intensity fluctuations arising due to motion of the scattering particle to the velocity of scatterers. This is done by measuring the decorrelation time through the $g_2(\tau)$. In the present work, we do not emphasize extracting the decorrelation time but focus more on the frequency spectrum of all the motion contributing to the measured intensity fluctuations. This is because in the present experiment, there are more factors leading to the fluctuation of intensity than the motion of the fluid alone. Based on the correlation models, the degree of variation can be converted to a correlation coefficient. To do so, we measure correlation coefficient for each frame [18]:

$$cc = \frac{\sum_{m=1}^N \sum_{n=1}^N (f_{mn} - \bar{f})(g_{mn} - \bar{g})}{\sqrt{\sum_{m=1}^N \sum_{n=1}^N (f_{mn} - \bar{f})^2} \sqrt{\sum_{m=1}^N \sum_{n=1}^N (g_{mn} - \bar{g})^2}}, \quad (5)$$

where $f_{mn}(m, n = 1..N)$ is the raw image intensity for a given pixel in a frame which is correlated with the raw image intensity for a given pixel in a subsequent frame g_{mn} . Here N is indicating the number of pixels in a frame row or column, which is equal in the present experiment. This is calculated for the entire time sequence. The average value for each matrix is denoted by \bar{f} and \bar{g} respectively. The two dimensional correlation coefficients have been calculated for all the pixels in the speckle image data and result in a value ranging from 0 (uncorrelated) to 1 (fully correlated). As the particles scatter more, the signal fluctuation increases and the average correlation value decreases. Applying the correlation approach for the speckle measurements can be limited as it depends on the resolution of the system and the amplitude of the motion. In case the speckle motion between successive frames falls into only a fraction of a pixel, a better sampling rate and higher resolution would be required to use the correlation approach. To track the temporal movement of the speckle pattern due to the pulsation signal

and the simulated motion, a series of images have been recorded and analyzed, for different settings, using this technique. For applicability to compact devices, we also studied the statistical correlation between the intensity fluctuations at two pixel locations for the time sequence of images from a measurement.

3. Results and discussion

In this section, we study the effect of different configurations of the flow cell on the fluid pulse as seen by the speckle images. As mentioned before, the flow cell has the option of variable volume or a rigid configuration. This results in different optical signatures captured by our system because the fluid pulsation in the two cases is different. We compare the speckle contrast data with correlation data obtained for measurements with both configurations of the flow cell.

3.1. Pulse shape

In order to simulate the in-vitro heart rate, we generate pulses at the rate of 1Hz in milk using the roller pump. To study the behavior of the simulated signal, the measurements have been done on the flow sample using the rigid and flexible channel. In the case of a rigid channel, we are only monitoring the laser speckle contrast variation with respect to velocity changes caused by the roller pump. In comparison, in the flexible setting we are adding one more variable which is the variation of fluid volume. The results of the measurements are shown in Fig 3. On the top panel of the figure, the fluctuation of speckle contrast of the pulse flow in a rigid channel is shown in time and spectral domain. It can be seen that there are harmonics of the main frequency of pulsation (1Hz). This is due to the pulse generated with the roller pump having a square shape.

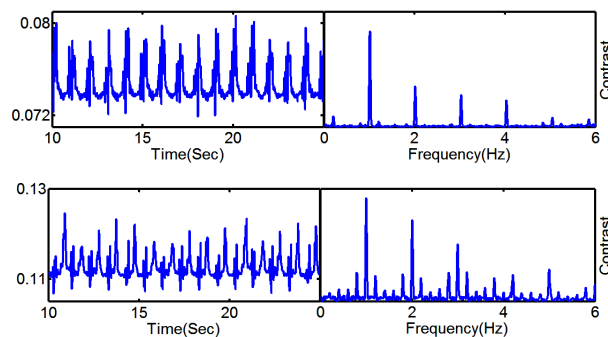


Fig. 3. Speckle contrast variation in time and spectral domain is shown for a milk pulsation of 1Hz for a rigid (upper plot) and flexible channel (lower plot).

The lower plot in Fig 3 shows the fluctuation of speckle contrast of the pulse flow in a flexible channel both in time and spectral domain. By comparing the result of both measurements, we notice the effect that volume change has. There is an additional modulation in the signal visible in the lower plot. These measurements have been done using a 1mm thick Delrin window as the top membrane. In order to show the influence of scattering medium on the measured signal, another series of measurements have been done with glass window, which contains no static scatterers, on top. The figure 4 shows the effect of the top layer for speckle contrast (left panel) and correlation based analysis (right panel). Based on both approaches, we can see a more clear signal using glass as the top membrane (upper plot) while the signal appears to be more distorted using Delrin (lower plot). In both figures, the variation in amplitude arises due to the different materials being used for the different configurations. In the following measurements

mentioned in the next section, the same configuration was used for the flow cell to ensure uniformity.

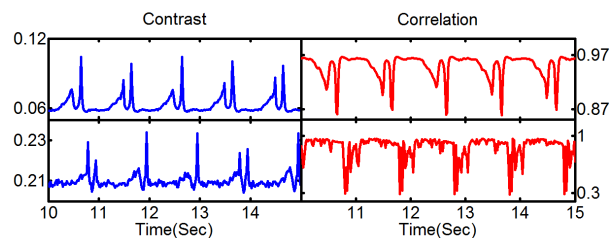


Fig. 4. The effect of medium is shown for milk pulsation of 1Hz using glass (upper plot) and Delrin (lower plot) based on a) speckle contrast and b) correlation analysis.

3.2. Induced motion artifact

To study the effect of additional perturbation on the optical signal from the scatterers due to relative motion between light source and flow sample, several experimental configurations were studied. The flow pulsation frequency was kept at 1.25 Hz and represents the main heart rate signal to be detected. The flow cell was kept in the rigid configuration to avoid the extra oscillations seen in the case where the volume is allowed to change. The top layer was Delrin with its skin-like scattering properties. The motion artifact was generated by using the shaker to move the laser at different frequencies (0.7Hz, 1.4Hz, 2.8Hz, 3.2Hz, 3.6Hz, 4Hz and 4.5Hz) with different amplitudes (0.5mm, 1mm, 2mm and 3mm). These measurements were then analyzed using the contrast and correlation formalisms mentioned earlier in the paper.

Out of these measurements, we show only the extreme cases, *i.e.*, at the frequency of 0.7Hz with 0.5mm and 3mm amplitude and at the frequency 4.5Hz with 0.5mm and 3mm in Fig 5 and Fig 6. The rest of the measurements show the same trend as seen for the extreme cases. The measurements were also performed at two different angles, 70° and 20° of the illumination laser with the camera, which is placed directly above the sample. The results of measurements at 70° are shown in Fig 5 and 20° in Fig 6. To study the impact of the camera exposure time on the measurements, we measured for exposure times of 20ms, 16ms, 8ms and 4ms, as shown in Fig 5 and Fig 6, in the panels a), b), c) and d), respectively. These correspond to camera frame rates of 50fps, 60fps, 125fps and 250fps, respectively.

The figures 5 and 6 show the results of the measurements using both analysis techniques after being smoothened and low pass filtered at 10Hz. It can be observed that we are able to differentiate the fluid pulsation rate from the induced motion effects. However, the spectral composition of the signal extracted from the temporal analysis of the contrast and correlation measurement exhibit some major differences. The spectrum obtained from this speckle contrast technique appears cleaner due to the extensive spatial averaging. The spectrum from the correlation analysis is more sensitive to fluctuations and more detailed. The contrast analysis mainly measures the double frequency of the induced motion as contrast analysis cannot distinguish the difference of the direction of laser motion. Speckle contrast analysis provides good visibility specially for low amplitude and frequency of laser motion. Increasing the amplitude and frequency of laser motion decreases the signal visibility for the contrast analysis for longer exposure times. Longer exposure times lead to more averaging and thus averages out the weaker optical signal from the flow pulse and emphasizes the laser motion. However, the performance using contrast analysis for higher frequencies is better for shorter exposure times of 8ms and 4ms. This result cannot be improved further without decreasing the spectral resolution of the data set unless the

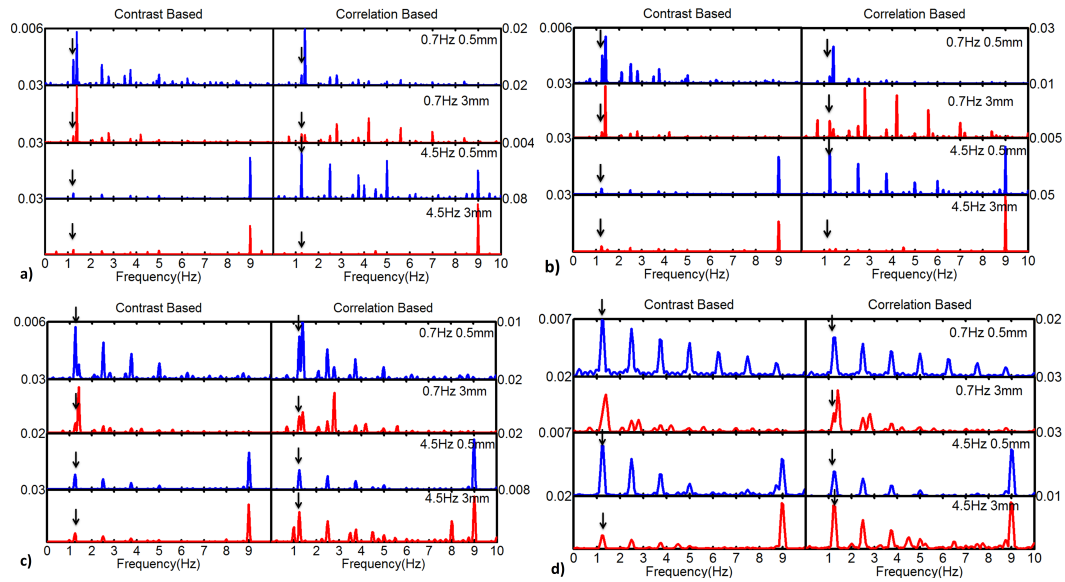


Fig. 5. Spectral analysis is shown for two displacements of the illuminating laser with an angle of 70° with the camera: 0.5mm (blue line) and 3mm (red line) displacement amplitudes and at the frequencies of 0.7Hz and 4.5Hz measured with exposure times of a) 20ms, b) 16ms c) 8ms and d) 4ms. The plot shows the result of measurements using the correlation analysis (right panel) and speckle contrast (left panel) for milk pulsation at 1.25Hz. The y-axis shows the amplitudes of the correlation analysis and speckle contrast on the right and left side of each panel, respectively.

recording time is increased or a smaller area of the camera chip is used. In comparison, correlation provides a richer spectrum which has more features. The signal visibility in the case of higher amplitude and frequency is better for correlation based analysis of the measurements. This is more obvious for shorter exposure times. It can also be seen that for large amplitude, low frequency measurements, the correlation technique fails to pick up the correct spectrum of the induced motion. Mainly because the harmonics have a higher amplitude. This is again better for the shorter exposure times.

The measurements done with a 70° angle of the illumination laser with the camera show better signal than the 20° measurements. The 70° configuration has a larger elongated illumination spot leading to a bigger area contributing to the speckle pattern on the detection plane. Also, there is more uniformity of illumination over the spot being studied. This can explain the reason for the observed difference. In the measurements mentioned above, the direction of motion of the laser is the same as the direction of flow, since this is the worst case scenario. The case where the flow direction was perpendicular to the laser motion was also measured and analyzed for all the configurations shown above. These results are omitted since no discernible differences are seen in comparison to the case shown above, where the flow and motion directions are parallel.

3.2.1. Pixel based analysis

For some device applications, the need for compactness and lower cost is imperative, therefore a trade-off between speckle image size and measurement sensitivity comes into play. For these applications, we decided to analyze our measurements using two groups of 2×2 pixels, positioned at locations opposing each other, across the beam diameter. The distance between the

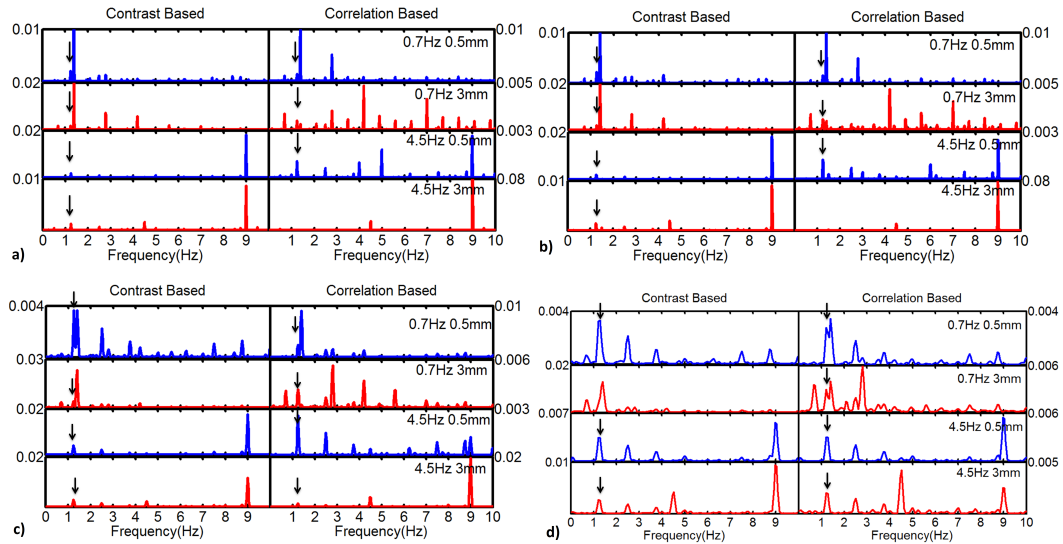


Fig. 6. Spectral analysis is shown for two displacements of the illuminating laser with an angle of 20° with camera: 0.5mm (blue line) and 3mm (red line) at the frequencies of 0.7Hz and 4.5Hz measured with exposure times of a) 20ms, b) 16ms c) 8ms and c) 4ms. The plot shows the result of measurements using the correlation analysis (right panel) and speckle contrast (left panel) for milk pulsation at 1.25Hz. The y-axis shows the amplitudes of the correlation analysis and speckle contrast on the right and left side of each panel, respectively.

super-pixels thus varied according to the beam size, in the two cases of the 70° and 20° configurations of measurement and was typically, 150 and 100 pixels, respectively. These super pixels mimic independent local detectors and were chosen in direction parallel to and perpendicular to the axis of motion of the laser. The result of this analysis has been shown in Fig 7. In this figure, the analysis result for both parallel and perpendicular directions of motion for 0.7Hz and 4.5Hz with the minimum and maximum displacement amplitude of 0.5mm and 3mm, is shown. The exposure time for each frame shown in Fig 7 was 8ms.

In Fig 7, we see that for low amplitude of displacement of the laser, two super-pixels are sufficient to measure the motion and the fluid pulsation using the correlation coefficients of speckle intensity. However, for higher amplitudes of laser motion the position of the super-pixels or in a device the detectors, with respect to the motion between the sensor and the subject, can play a significant role in the measurement results. In case of a parallel configuration of the super-pixels with respect to the laser motion, only the induced motion is detected when the laser motion is large.

3.3. Measurement in-vivo

The measurement was implemented in-vivo by placing the finger of a volunteer in the place of the flow cell. To verify the measurements, the volunteer also wore a commercial pulse oximeter on the thumb. The analog signal from the pulse oximeter was synchronized with the camera frames recorded for the measurement. The results of the measurements can be seen in Fig 8 for the three different motion frequencies of the illuminating laser (1Hz, 1.4Hz and 2.8Hz) and at two different amplitudes of 0.5mm and 0.8mm. To keep the heart rate values similar, the measurements for the low amplitudes of the shaker (0.5mm) were performed for all the

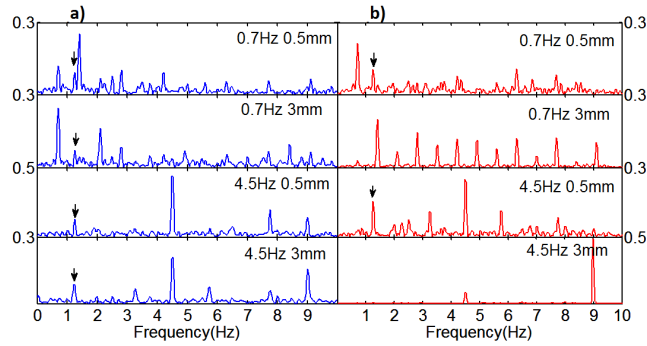


Fig. 7. Spectral analysis for pixel correlation is shown for frequencies of 0.7Hz and 4.5Hz with displacement amplitudes of 0.5mm and 3mm after being analyzed in a) perpendicular and b) parallel directions to the induced motion artifact. In each plot, the arrow points at the fluid pulse rate. The y-axis shows the amplitudes of the parallel configuration and perpendicular configuration on the right and left side of each panel, respectively.

frequencies of motion and being followed by the higher amplitude of displacement (0.8mm). The measurements were performed for 20ms exposure time.

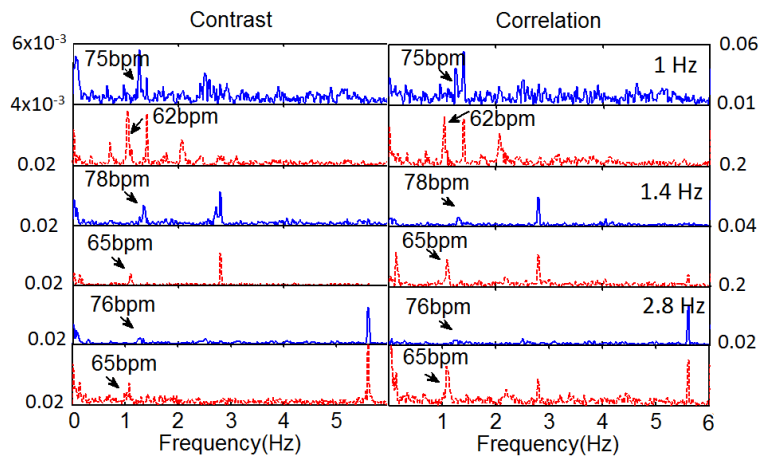


Fig. 8. Spectral analysis is shown for the measurement with human finger for two displacements of the illuminating laser: 0.5mm (blue line) and 0.8mm (red line) measured with correlation analysis (right panel) and speckle contrast (left panel). The y-axis shows the amplitudes of the correlation analysis and speckle contrast on the right and left side of each panel, respectively.

The results can be seen in Fig 8 and confirm our expectations from the in-vitro measurements that the detectability of the signal drops for higher motion amplitudes and frequencies using the speckle contrast approach. The correlation method measures a higher signal amplitude and is more robust to high-amplitude laser motion. Based on the speckle contrast, the signal visibility decreases at larger displacements of the laser while the sensitivity of correlation analysis stays in a comparable range and gives a higher signal visibility.

4. Conclusion

In this paper, we study a system based on dynamic light scattering and techniques to extract physical parameters of the scatterers. This was done specially for pulsatile flow in face of motion induced artifacts. Measurements for a full parameter set, including different amplitudes and frequencies for motion of the illumination, alignment configurations of illumination and detection, and camera exposure time were carried out. This measurement data was then analyzed with different analysis techniques based on speckle contrast and correlation. In general, we observed that, correlation based analysis is more robust against high amplitude laser motion, particularly when combined with short exposure times. Also, a larger angle between illumination and detection yields a better signal. Measurements were also performed on the finger of a volunteer and analyzed using the two techniques. The in-vivo measurement results agreed with the results of the in-vitro case. The measurements were analyzed again using only a few pixels from the entire camera image to mimic independent local detectors. It was observed that a few pixels from the image were sufficient to extract the necessary parameters, which is useful in case of compact devices. Therefore, we conclude that several speckle based techniques, can be used to understand the effect of motion induced artifacts. These studies can be incorporated in future devices to make them more robust.

Acknowledgments

This work was funded by AgentschapNL under the project IOP Photonic Devices, IPD083359 HIP - Hemodynamics by Interferometric Photonics. The skin perfusion phantom has been developed by L.G. Paroni and J. M. A. Stijnen from LifeTec, Eindhoven. The authors would also like to express gratitude to R. C. Horsten, T. Zuidwijk, R. Pols of TUDelft for their help and support with the experimental setup.